UPPSALA
UNIVERSITET

FREIA Report 2016/1
Jan. 2016

DEPARTMENT OF PHYSICS AND ASTRONOMY
UPPSALA UNIVERSITY

RF Test of the ESS Double Spoke Cavity

H. Li, V.A. Goryashko, A. Bhattacharyya, R. Ruber

Uppsala University, Uppsala, Sweden

Department of
Physics and Astronomy
Uppsala University
P.O. Box 516
SE – 751 20 Uppsala
Sweden

Papers in the FREIA Report Series are published on internet in PDF format.
Download from http://uu.diva-portal.org

RF Test of the ESS Double Spoke Cavity

H. Li, V.A. Goryashko, A. Bhattacharyya, R. Ruber

Uppsala University, Uppsala, Sweden

Abstract

A bare spoke cavity has been tested at FREIA Laboratory with a Self-exited loop at low power level to confirm its vertical test performance at IPNO. Similar test results as IPNO's previous test were obtained with FREIA system. This report presents the details of each measurement.

Table of Contents

1. Introduction 5

2. Design of the ESS spoke cavity 5

3. SEL test stand and calibration procedure 7

4. Measurement of the resonance frequency 8

5. Gradient Measurement 9

6. Residual Resistance 14

7. Pressure Sensitivity 15

8. Lorentz Force Detuning 17

9. Microphonics 23

10. Tuner sensitivity 24

11. Summary 27

References 27

1. Introduction

ESS, the European Spallation Source, will be an accelerator-driven facility contributing for academia and industry scientific research topic using neutron beams. The project started construction in 2013 aims to deliver first neutrons in 2019 [1]. The linear accelerator, or linac, is thus a critical component. The superconducting spoke section of the linac accelerates the beam from the normal conducting section to the first family of the elliptical superconducting cavities. This section adopts a single family of bulk niobium spoke cavities, a total of 26 spoke cavities, grouped by 2 in 13 cryomodules [2]. The choice of the spoke resonator is driven by the potential for high performance at low/middle energy part and intrinsic mechanical advantages. As a new resonator structure, only about 15 spoke prototypes of different types and β's have been fabricated and tested worldwide. However, many high power proton accelerator facilities are currently considering adopting spoke technology. The ESS linac will probably be the first to be constructed with spoke cavities. Therefore, developing of spoke cavities becomes one of the most important parts of the whole project.

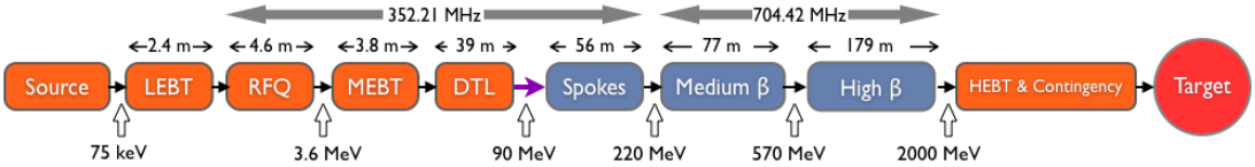

Figure 1: The layout of ESS linac

The FREIA laboratory (Facility for Research Instrumentation and Accelerator Development) at Uppsala University is established in order to support the development of instrumentation and accelerator technology [3]. The key project of FREIA is developing the ESS superconducting spoke linac. This project contains three phases: (1) test of the first RF source, (2) test of the prototype cavity and (3) test of the prototype cryomodule [4]. In the second phase, the bare spoke cavity will be tested at low power level to confirm its vertical test performance at IPNO. Then the spoke cavity with a RF power coupler will be tested at high power with the tetrode amplifier based RF system from phase 1. Since a self-exited loop has a lot of advantages for testing high gradient, high-loaded Q cavities. FREIA developed a test stand based on a self-exited loop for demonstrating the performance of superconducting cavity at low power level. One of the ESS spoke cavity prototype, Germaine, has been tested in 2015 with the FREIA system and similar test results as IPNO's previous test [5] were obtained.

2. Design of the ESS spoke cavity

ESS linac will include a single family of β=0.5 bulk niobium double spoke cavities, operating at a temperature of 2 K, and at a frequency of 352.21 MHz. A total of 26 Spoke cavities, grouped in pairs in 13 cryomodules, will take up 56 m of length. The chosen operating accelerating field is 9 MV/m, where the accelerating length is defined to be $(n+1)\ \beta\lambda/2$, and n is the number of spoke bars. The required peak RF power to supply one cavity will be about 250 kW for the 62.5 mA beam intensity, corresponding to 10 kW of average power at a duty factor of 5% [6].

Table 1 main RF parameters of ESS double spoke cavity

Frequency [MHz]	352.21
Beta_optimum	0.50
Operating gradient [MV/m]	9.0
Temperature (K)	2
Bpk [mT]	61
Epk [MV/m]	38
G [Ohm]	133
r/Q [Ohm]	427
Lacc (=beta optimal x nb of gaps x λ /2) [m]	0.639
Bpk/Eacc [mT/MV/m]	6.8
Epk/Eacc	4.3
P max [kW]	335

Table 2 Frequency sensitivities of the cavity

Stiffness of the cavity [kN/mm]	20
Tuning sensitivity f/z [kHz/mm]	135
Sensitivity to helium pressure KP [Hz/mbar] Without CTS With CTS	 16.5 26
Lorentz detuning factor KL [Hz/(MV/m)^2] Without CTS With CTS	 -5.13 -4.4

The ESS spoke cavities are designed at IPNO. A numerical simulation analysis of the behavior of the cavity and helium vessel has been conducted, permitting the development of a mechanical design of the cavity with its stiffeners and the helium tank. The main parameters of the spoke cavities are shown in Table 1 and 2 [7]. Since March of 2013, three prototypes have been launched in production: one is manufactured by SDMS (France) and two others by ZANON (Italy), as shown in Figure 2 [8].

Figure 2: left #1 (Romea); middle #2 (Giulietta); right #3 (Germaine)

3. SEL test stand and calibration procedure

3.1 SEL test stand

The cryogenic testing of double spoke cavity Germaine was carried out at FREIA with a self-exited loop test stand, as shown in Figure 3. In the loop, the cavity is a narrowband filter and starts from noise to oscillate by itself. Only two constraints apply: the total loop phase must be a multiple of 2π and the gain of this positive feedback loop must be greater than 1. In this way, the cavity field amplitude is unaffected by the ponderomotive instability and there is no need for an external frequency source and tracking feedback. Therefore, the self-excited loop is ideally suited for high gradient, high-Q cavities operated in CW mode [9].

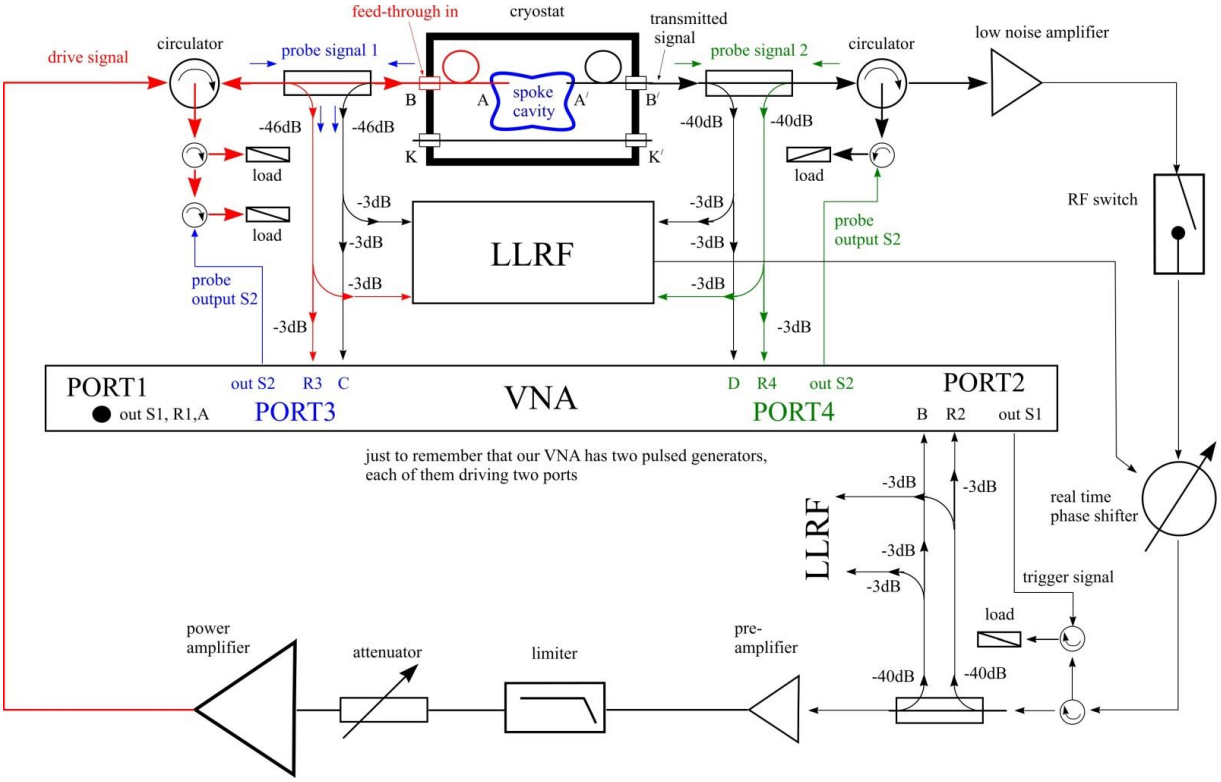

Figure 3 SEL setup at FREIA

We use a vector network analyzer (VNA) as receiver when running the SEL. To protect the system from radiation, the cavity is located at 20 m distance from the control and measure system. The function of the VNA in this loop is double fold: it provides a convenient cable calibration and can also be used as receiver in the measurement. This way of using the VNA gives us both true powers and the phase information of signals even beyond the equipment limits. We also developed a digital phase shifter and gain-controller, based on NI FlexRIO FPGA and NI 5782R data acquisition modules. With this digital system, we can vary the loop delay with high-precision, from that we obtain the reflection coefficient as a function of loop delay.

Before the ESS double spoke cavities, a single spoke cavity Hélène from IPNO has undergone cold tests with this loop to check our test method, hardware setup and cryo-system. Similar test results as IPNO's previous test show that this test stand is ready for superconducting cavities' low power test [10].

So far, some key parameters of SEL at FREIA are listed below:

- The maximum power around 100 W by using one commercial amplifier, up to 1 KW by one 352 MHz single ended demonstrator amplifier module ;
- The maximum gain of the loop can reach 120 dB ;
- 40 dB variable attenuation range depending on control voltage;
- 270 degree delay by a trombone phase shifter;
- High-precision loop delay and loop gain control can be obtained by a digital phase.

3.2 Calibration procedure

Two methods, by power meter and VNA, are adopted to double check the accuracy in the measurement. During all these measurements, two cavities are set inside the new HNOSS horizontal cryostat system at the same time [11]. Six identical cryo-cables are installed inside the cryostat, four connect to cavities ports and cryostat flange separately, while the other extra two cables connect back to back with a through as reference. Corresponding to different method, two calibration procedures are used to calculate true power going into or from the cavity. The procedure is based on the method that has been used on the single spoke cavity and the detail can be found in [12].

4. Measurement of the resonance frequency

During the RF measurements, resonance frequencies of Germaine in three different temperature situations have been studied. These results will help us with the frequency control during the cavity fabrication and post-processing. Note that in the first test of Germaine in June 2015, the pick-up antenna has been found to have a much higher external Q value, thus the mismatching between the cavity and input power led to the failure of the resonance frequency measurement at room temperature. Here, the results are gotten after the pick-up coupler was repaired, as shown in Table 3.

Table 3 Resonance frequency of Germaine

Temperature	Resonance frequency	Measure method
300 K	351.533 MHz	VNA S parameter measurement
4 K	352.038 MHz	Self-exited loop
2 K	352.032 MHz	Self-exited loop

5. Gradient Measurement

5.1 Measurement result

At the low power test, the double spoke cavity (Germaine) and the single spoke cavity (Hélène) are set inside the new HNOSS horizontal cryostat system at the same time. Both cavities are equipped with a fixed-length input antenna and a pick-up antenna. The low power test of Germaine started from June 2015 and lasted until shipping it back to IPNO in January 2016. In general, the measurements could be divided into three runs. The measured Q_0 as a function of accelerating gradient is shown in Figure 4, while the low-field Q_0 factor and external Q factor of the pick-up antenna are listed in Table 4.

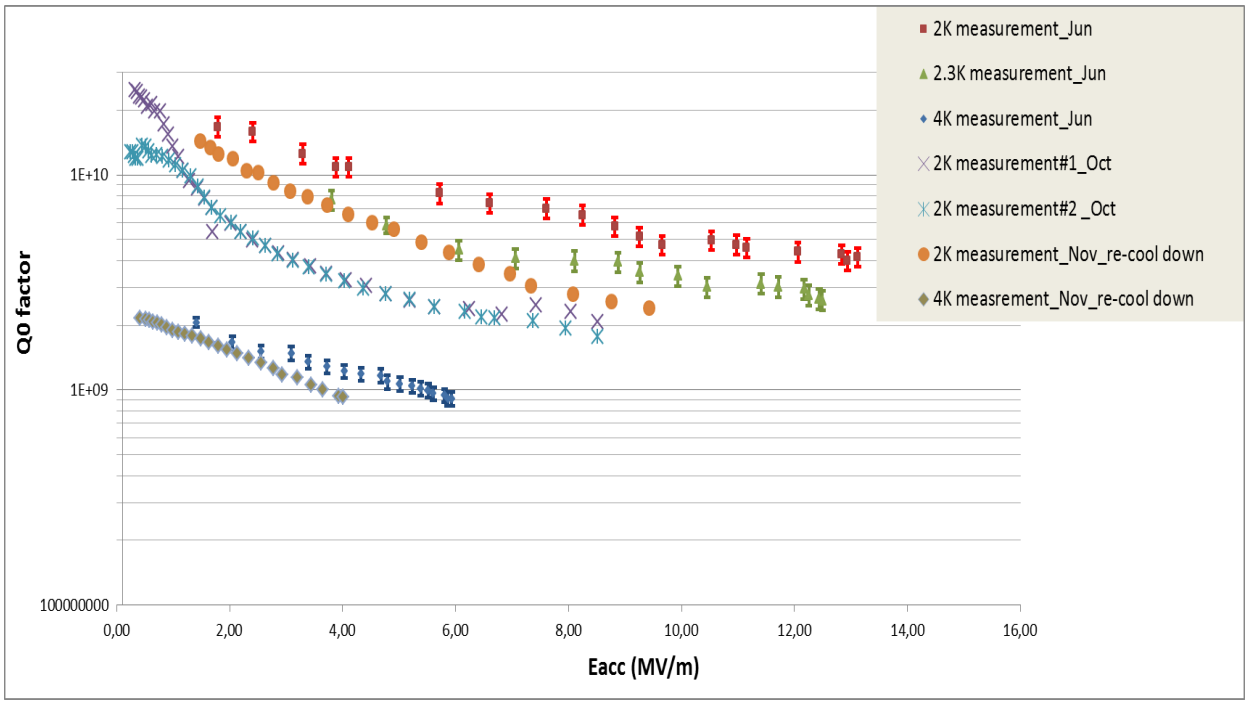

Figure 4 Q_0 factor as a function of accelerating gradient of Germaine at FREIA

Table 4 Different Q factors of Germaine in each run

Time	Q_0 factor at low field	Qt	comment
Jun.	1.7×10^{10}	9.2×10^{15}	Pick-up antenna was short with beam tube
Oct.	1.4×10^{10}	3.3×10^{11}	Antenna repaired
Early Nov.	4.5×10^{9}	1.2×10^{11}	Thermal cycle
Late Nov.	1.6×10^{10}	1.2×10^{11}	Re-cool down

The first run is performed on June, corresponding to cryostat run 5/A. The 4 K experiments were carried out first and followed by cool down to 2 K. During this cool down, frequency and Q_0 measurements are performed in order to measure pressure sensitivity and the residual resistance. Finally, the 2 K test is performed. By decay time measurement at 4 K, Germaine shows a Q_{in} of 1.6×10^{9}. The low-field Q_0 factor reached 1.6×10^{10} at 2 K and 2×10^{9} at 4 K, respectively.

We also found the problem of the pick-up antenna in this run. The external Q value is roughly in the order of 1×10^{16}, which is much higher than the design value 1×10^{12}. Such high Q_t led to super low transmitted power from the cavity, which requires a higher gain to run the loop also introduces a lot of noise into the system. Lots of multipacting barriers were encountered in the SEL and caused unstable situation at low field level. In order to pass them, we set the lowest attenuation in order to obtain the highest gain to amplify a small driven signal as quickly as possible. Once the loop has gone through a barrier, reflection goes down and forward power increases but is limited by limiters and the maximum amplifier output. In order to check the situation of the antenna, several tests have been performed. With a multimeter, we detected that the pick-up antenna was shorted with the cavity wall. The deformation or unscrewed connection of the antenna during the shipping would be the potential reasons. When we opened the cavity in a portable cleanroom in October, we checked the antenna and it was unscrewed and touched the cavity tube, then after fixing the antenna, we closed the cavity.

At the second run, corresponding to cryostat run 6/A, Germaine was retested at 2 K without any extra post processing. Before the RF measurement, we took more than an hour for conditioning. When there was a defect on the cavity internal wall, an electromagnetic field could much easily lead to a high surface field around this area which produced high x-rays. We set the loop phase in order to find a certain position that would keep a high radiation and degassing. Until the radiation goes down, then we sweep to another point. The radiation record shows that after the conditioning, radiation is back to the background, as shown in Figure 5. Also learn from the transmitted signal shown in Figure 6, the RF signal is disturbed at the beginning and then became a better sine waveform during the conditioning.

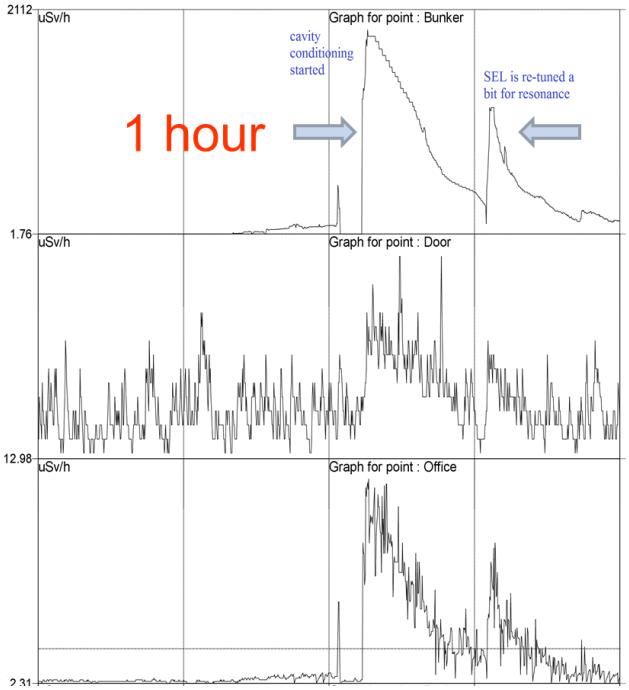

Figure 5 Radiation at different place during the conditioning

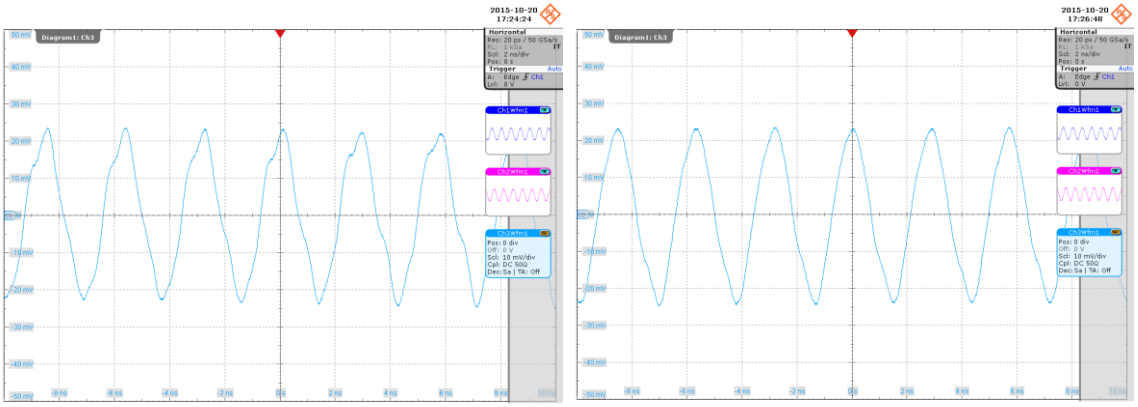

Figure 6: The transmitted signal waveform of Germaine: at the beginning of the conditioning(left) and after conditioning (right)

Then the Q_0 factor measurement was only performed at 2 K at this run. The blue and purple curves in the Figure 4 show that the performance of cavity decreases significantly. Due to the Q-slop curve dropped down quickly at low fields, we suspect a Q-disease rather than cavity pollution. Figure 7 shows that it was a fast cool down, 230 minutes from 290 to 4 K, the only thing we found from the record was the temperature warmed up to around 55 K for several hours just after Germaine cooled down. This temperature should be lower than the Q-disease region, but we are not sure how it affected the cavity. Several thermal cycles have been taken out under 20 K during this run in order to improve cavity performance, unfortunately, it was related to an even worse result.

Figure 7: Cool down curve of Germaine at the second run: whole curve (up) and the zoom in of cool down (down)

Finally, we warm up and re-cool down the cavity to check the cavity performance. Limited by the tight schedule, the last run was taken after re-cool down from 200 K. The cooling rate is shown in Figure 8. Note that the calculated cooldown rates are for a temperature range 150K >T >20 K and not since the starting point of the cooling. Average cooldown rate is 2.16 K/ min. Also all the cooldown rates are given as minimum values: since some temperature sensors are slow, the longest time periods in this temperature range for each cavity were taken. After re-cool down, the cavity's Q-slop improved much both at 2K and 4 K, but still did not reach the first-run result, as shown in Figure 4.

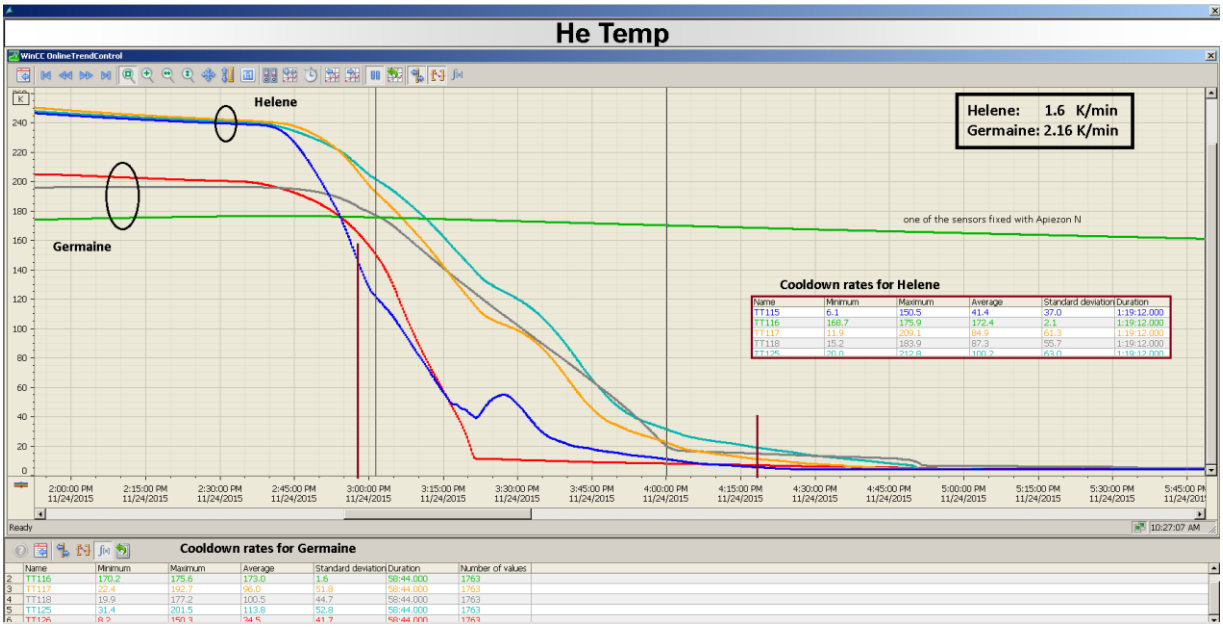

Figure 8: The cooling rate of Germaine at the third run

Figure 9 shows the comparison with the result of IPNO [8], Germaine still seems to be affected by Q-disease at this run, and some more post surface processing is need. After all, the results of 2 K test show that this double spoke cavity matches the ESS requirement of 1.5×10^{9} @9MV/m.

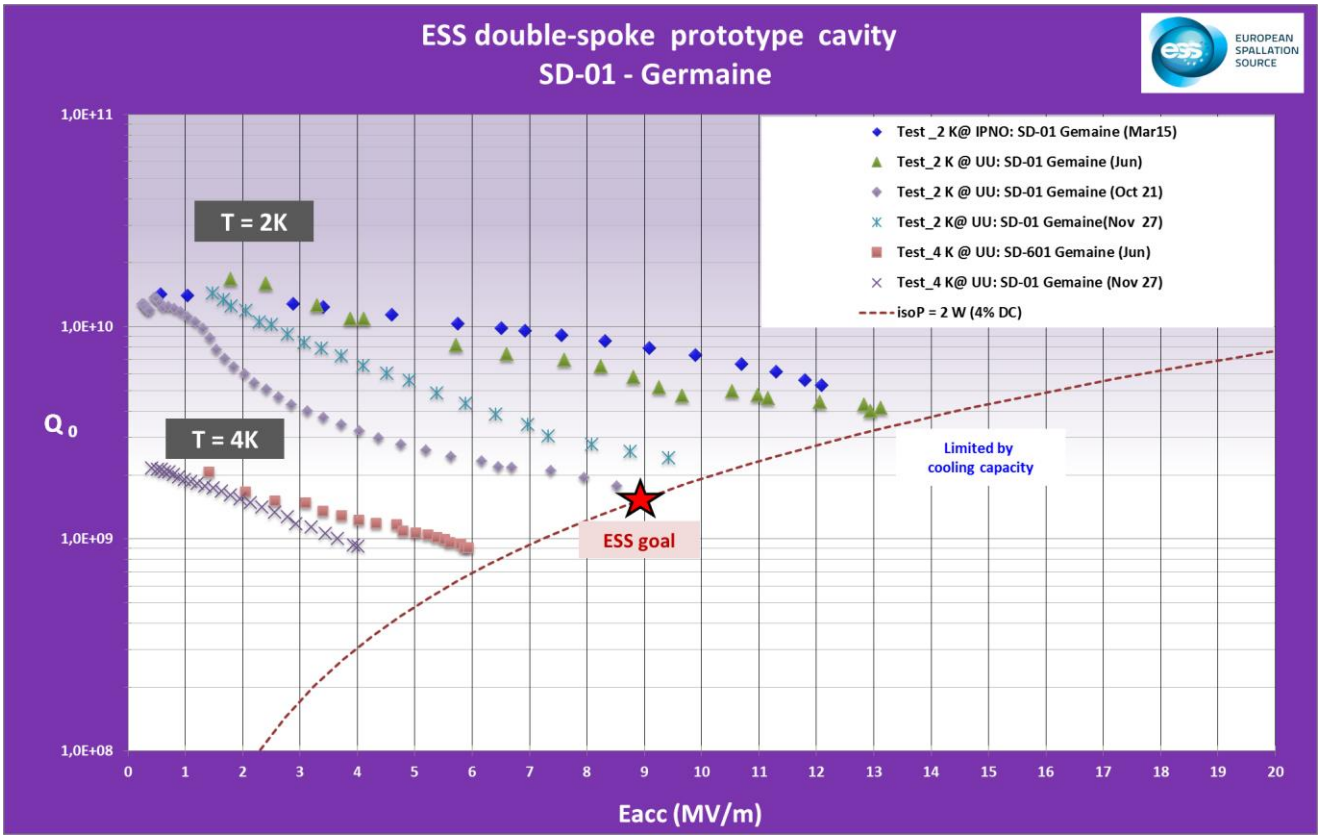

Figure 9: Q_0 factor as a function of accelerating gradient of Germaine

5.2 Q-surface method

We also develop a high-precision method for measuring a quality factor Q_0 of superconducting RF cavities as a function of the cavity voltage. The standard Q factor measurement suffers from a deficiency originating from a single data point measurement of the reflection coefficient. Typical uncertainty of Q_0 found in this way is 10-15%. With a Q-surface method, we improve the accuracy by an order of magnitude.

In order to obtain the Q-surface, for fixed forward power to the cavity we change step-by-step the phase shift across the cavity by tuning the digital phase shifter installed in the loop. This procedure is performed for each power level of interest, yielding the complex reflection coefficient of the cavity as a function of the cavity voltage and phase shift. The original data is shown in Figure 10 as a 3D plot. The measurement points with close values to the cavity voltage are grouped into slices and each slice forming a circle is used to deduce more accurate calculation of Q_0 the circle radius by means of the least-square minimization. All details of this method can be found in [13].

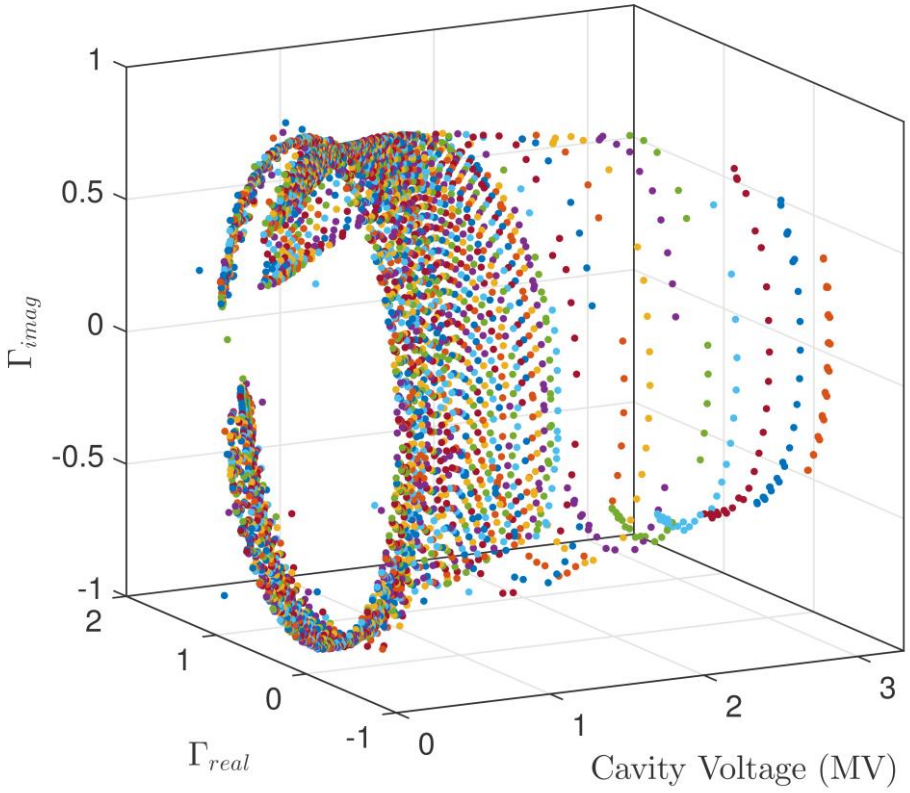

Figure 10 The real and imaginary parts of reflection coefficient vs. cavity voltage.

6. Residual Resistance

The surface resistance of a niobium superconducting cavity is the sum of the BCS (Bardeen-Cooper-Schrieffer) surface resistance and the residual resistance, which fulfils [14]

$$R_s = R_{BCS}(T) + R_{res} \quad (6.1)$$

On the other hand, the formula $G=Q_0 \times R_s$, where G is the so-called geometry factor, depends only on the cavity shape and R_s could be determined by measuring the Q_0 factor as a function of temperature. The surface resistance vs temperature curve at a fixed gradient is taken during cool down from 4 K to 2 K and is shown in Fig. 11. Here, the BCS resistance is calculated by the approximated formula given by equation 4.43 in Ref [15].

$$R_{BCS}(T, f) = \frac{A}{T} f^2 \exp\left(-\frac{\Delta}{k_b T}\right) \quad (6.2)$$

Since the data below 100 mbar failed to be saved in the first measurement, the preliminary result of the surface resistance is above 2.5 K. In this measurement, the residual resistance of Germaine is no more than 15 nΩ.

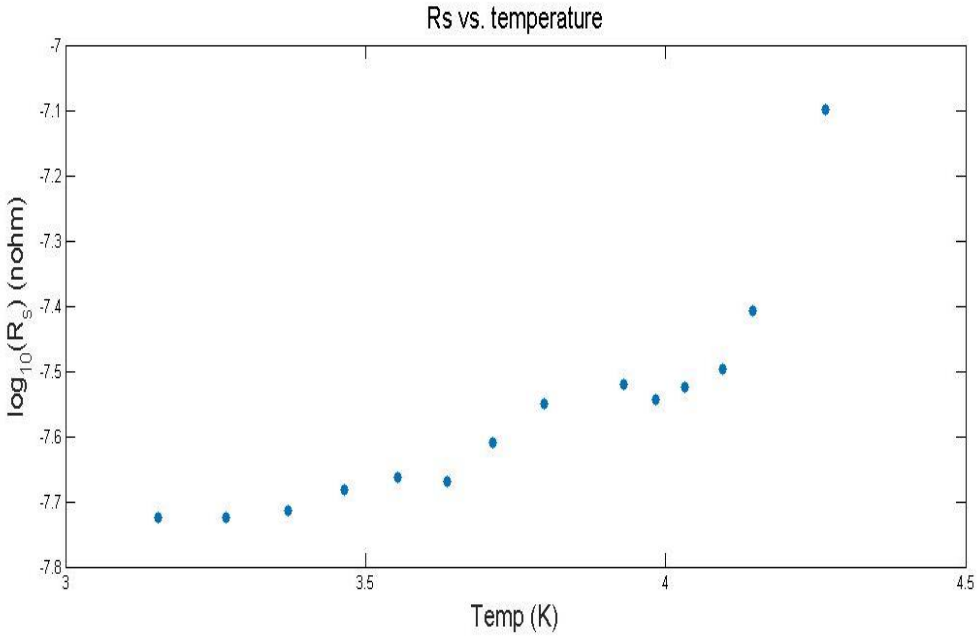

Figure 11 Rs vs. T measurement of Germaine at fixed gradient @ 2 MV/m

7. Pressure Sensitivity

Helium pressure fluctuation in the tank is one of the main sources of cavity resonance frequency detuning. Measuring the frequency sensitivity to the helium pressure provides information on the mechanical stability of the cavity. There are several ways to carry out cavity mechanical stability measurements. One direct way is to measure the frequency shift while monitoring transient pressure at the same time. Another simple way is to measure the resonance frequency shift when cooling down from 4.2 K to 2 K while the helium pressure is reduced from roughly one bar to 30 mbar.

Figure 12 shows how the helium pressure and resonant frequency of the cavities drift over a certain period. Note that the cavity vessel is fixed on a table by four points inside the cryostat and cavities are tested without a tuning system.

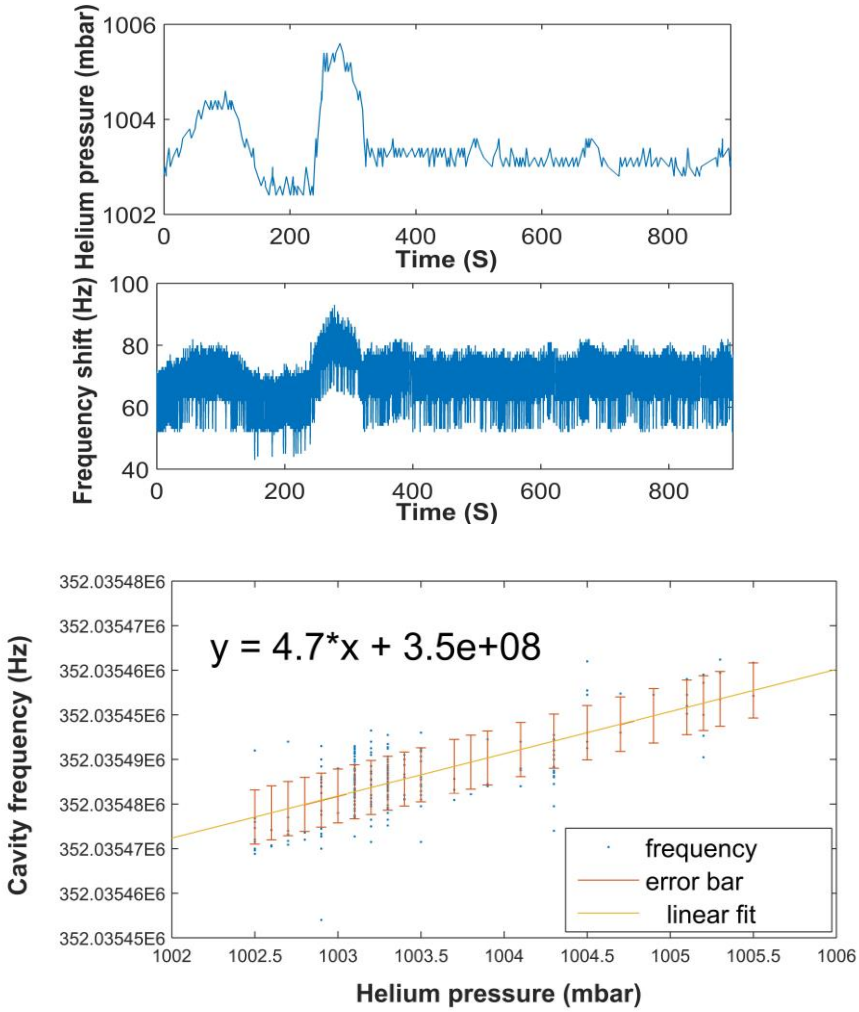

Figure 12 pressure sensitivity of Germaine, where top and middle graphs are the helium fluctuation and frequency shift, respectively.

In the measurement we determined that the ESS double spoke cavity has a pressure sensitivity of +4.7 Hz/mbar, while the test result of IPNO is +5.5 Hz/mbar. This result is consistent with the 5 kHz frequency shift measured during cool down from 4.2 K to 2 K and the corresponding pressure reduction from 1000 mbar to 30 mbar. In this way, the frequency sensitivity can be figure out by equation (7.1).

$$frequency \quad sensitivity \quad (Hz/mbar) = \frac{f(4.2K) - f(2K)}{pressure(4.2K) - pressure(2K)} \qquad (7.1)$$

Note that the mechanical contraction from 4K to 2K is very small, thus frequency shift cause by temperature can be ignored. Just a small and stable RF input power is used to track the cavity resonance frequency.

8. Lorentz Force Detuning

8.1 Static Lorentz force detuning

For a pulsed machine like ESS, Lorentz force detuning is an important role of resonant frequency detuning. RF power deforms the walls of the spoke cavities, which generally results in a reduction of resonant frequencies. The frequency shift is proportional to the square of the accelerating field and the proportionality constant K_L is the Lorentz force detuning coefficient, which fulfill the following equation (8.1):

$$K_L \quad (Hz/(MV/m)^2) = \frac{\Delta f}{\Delta E^2} \quad (8.1)$$

Therefore, the effect of Lorentz detuning must be taken into account in order to achieve higher accuracy of resonant frequency control.

Two static Lorentz force detuning tests of the ESS double spoke cavities have been performed at FREIA. In this section, the test method and result are presented below.

8.1.1 Standard method

Firstly, as a traditional way, we track the frequency shift with a spectrum analyzer while increasing the field. When measuring the static Lorentz force detuning, the spoke cavity is kept at different power levels over a certain period while keeping track of the helium pressure. Then, the frequency shifts for different accelerating gradients at the same pressure situation are recorded for analysis. Another way is considering helium liquid fluctuation as a background noise source, scan the cavity frequency over a long period in the Lorentz detuning measurement, then take away the effect of the pressure fluctuation by means of averaging the instant frequency.

The static Lorentz force detuning measurement of Germaine has been measured twice at FREIA. Figure 13 shows the result before repairing the pick-up coupler. In this run, the static Lorentz force factor -2.7 Hz/(MV/m)² is lower than those obtained through simulations, a difference which we attribute to the mechanical support of the cavities in the cryostat.

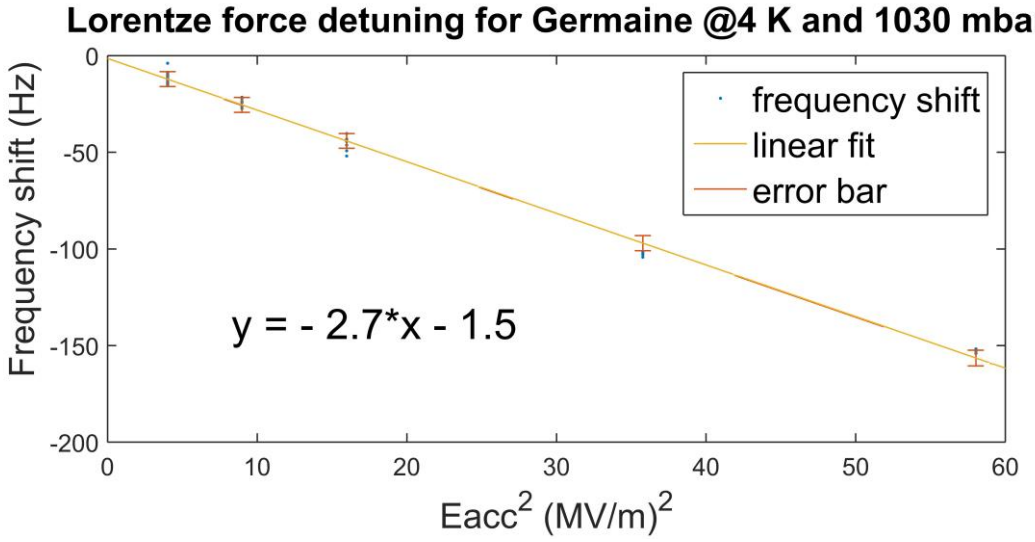

Figure 13: static Lorentz detuning curve of Germaine at first run

After fixing the antenna, we loosed one screw between the cavity and the support table in the cryostat in order to decrease the mechanical restriction to the cavity. The same measurement was repeated at 2 K and the results are shown in Figure 14 and 15, respectively. A static Lorentz force factor of -7.4 Hz/(MV/m)² in this run is very closed to the value of IPNO of -8.1 Hz/(MV/m)².

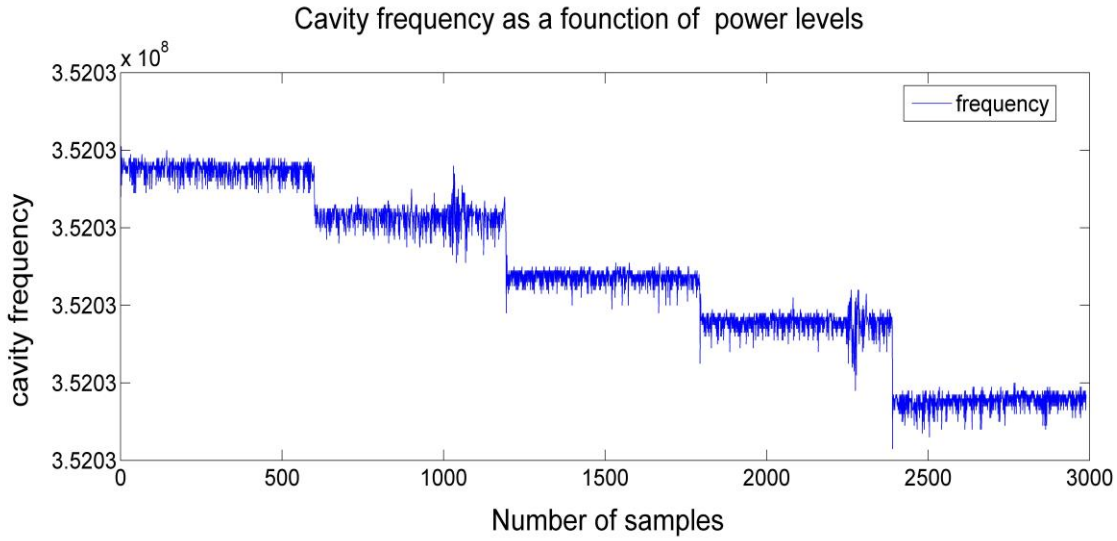

Figure 14: cavity frequency at different power level over a long period

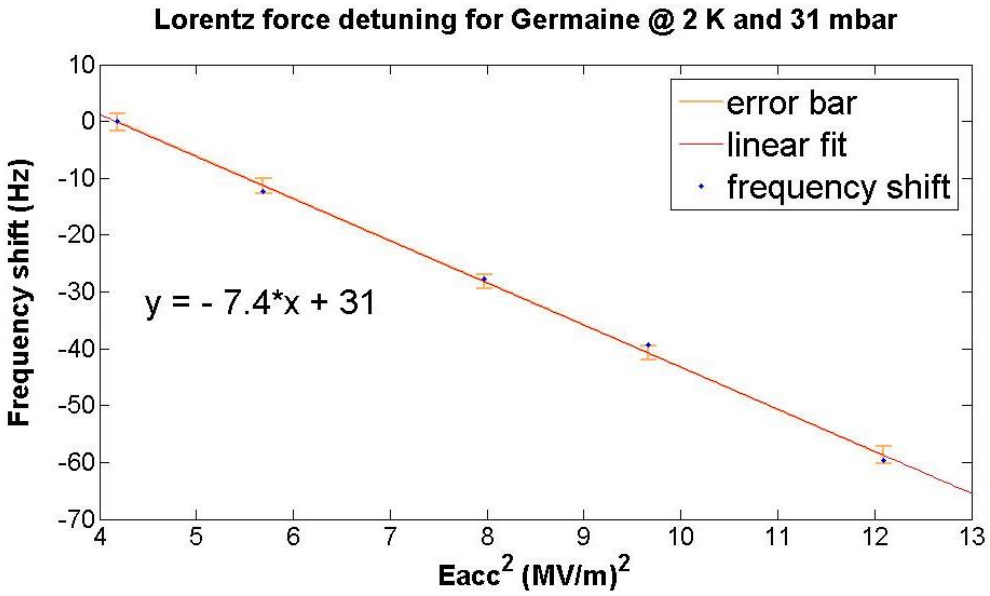

Figure 15: static Lorentz detuning curve of Germaine after pick-up coupler repaired

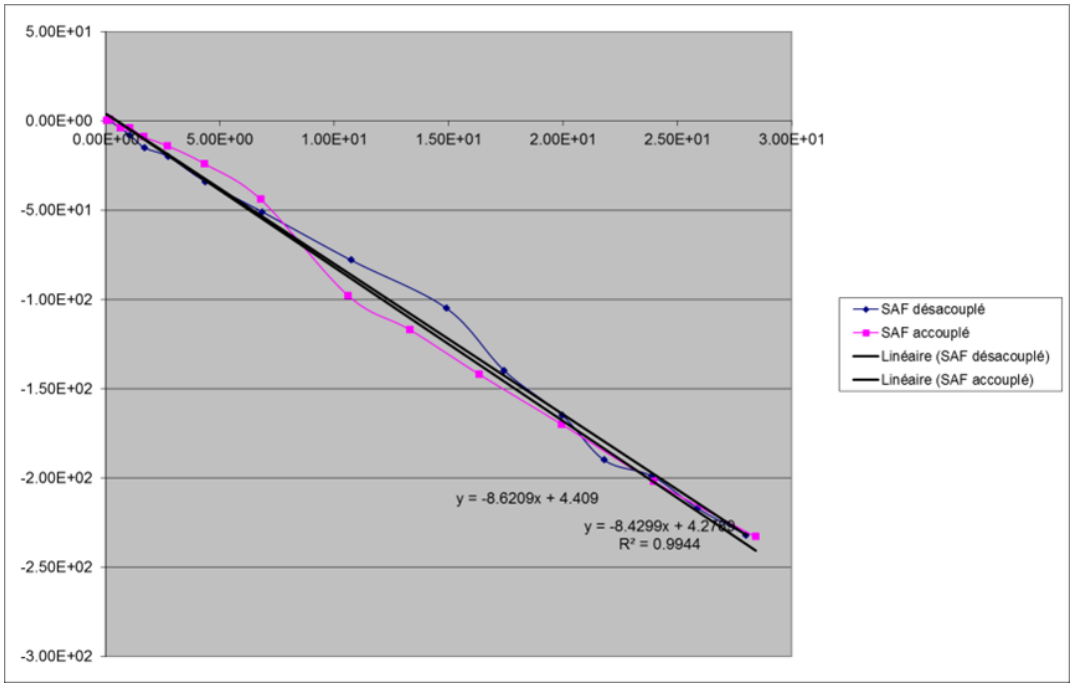

Figure 16: static Lorentz detuning curve of Germaine of IPNO

8.1.2 Cavity voltage modulation

We also developed a gain-controller, based on NI FlexRIO FPGA and NI 5782R data acquisition modules. By using the NI system in the loop, we stimulate the cavity by amplitude modulation with a low frequency by an order of 0.1 Hz. The choice of such low modulation frequency since it is well below the mechanical modes of the cavity then all mechanical modes are excited quasi-statically. As shown in Figure 17, there is no resonance of 0.1 Hz was simulated in the microphonics spectrum. That means that the Lorentz force changes on a time scale much longer than the characteristic time of the mechanical modes and retardation of the mode response can be neglected, the mode is assumed to react instantaneously to the cavity voltage $\Delta\omega \propto |V|^2$. The longer the modulation period, the better approximation works. However, for longer modulation periods fluctuations of helium pressure start to play a stronger role and distort measurements, finally, the period is set to 0.05 Hz.

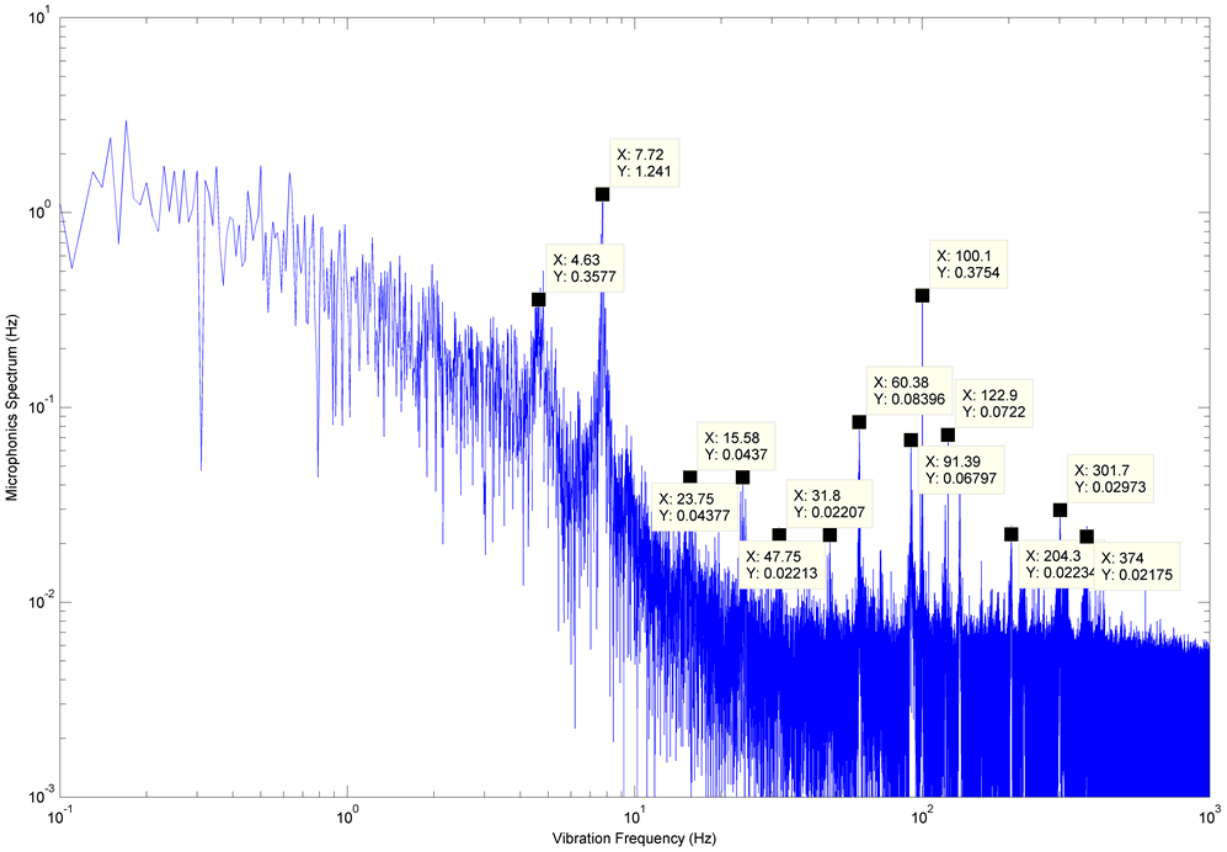

Figure 17 Microphonics spectrum of double spoke cavity with 0.1 Hz amplitude modulation.

By running the cavity for a reasonably long time period, for example of 1000 sec, and fitting a sine function to the cavity voltage and frequency. We then detect the cavity frequency deviation with a built-in I/Q demodulation set in a Rohde & Schwarz (RTO 1024) oscilloscope. The ratio of the cavity frequency modulation amplitude to voltage modulation amplitude squared gives the Lorentz force detuning coefficient.

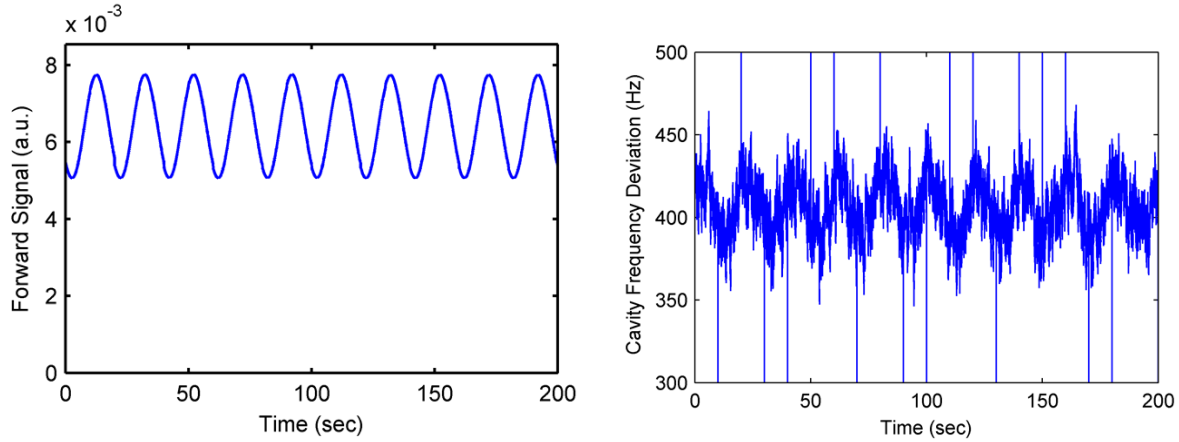

Figure 18 Variation of the cavity voltage (left) and frequency upon amplitude modulation of forward power (right).

The response of cavity forward signal and the instant resonant frequency while using 0.05Hz voltage modulation at 2 K are shown in Figure 18. Performing the Fourier transform of the instant resonant frequency, one gets the average peak-to-peak frequency modulation of approximately 15.87 Hz, as shown in Figure 19. Here according to the cavity signal, the corresponding accelerating gradient changes of 2.3 $(MV/m)^2$. That gives a Lorentz force detuning coefficient of -6.8 $Hz/(MV/m)^2$.

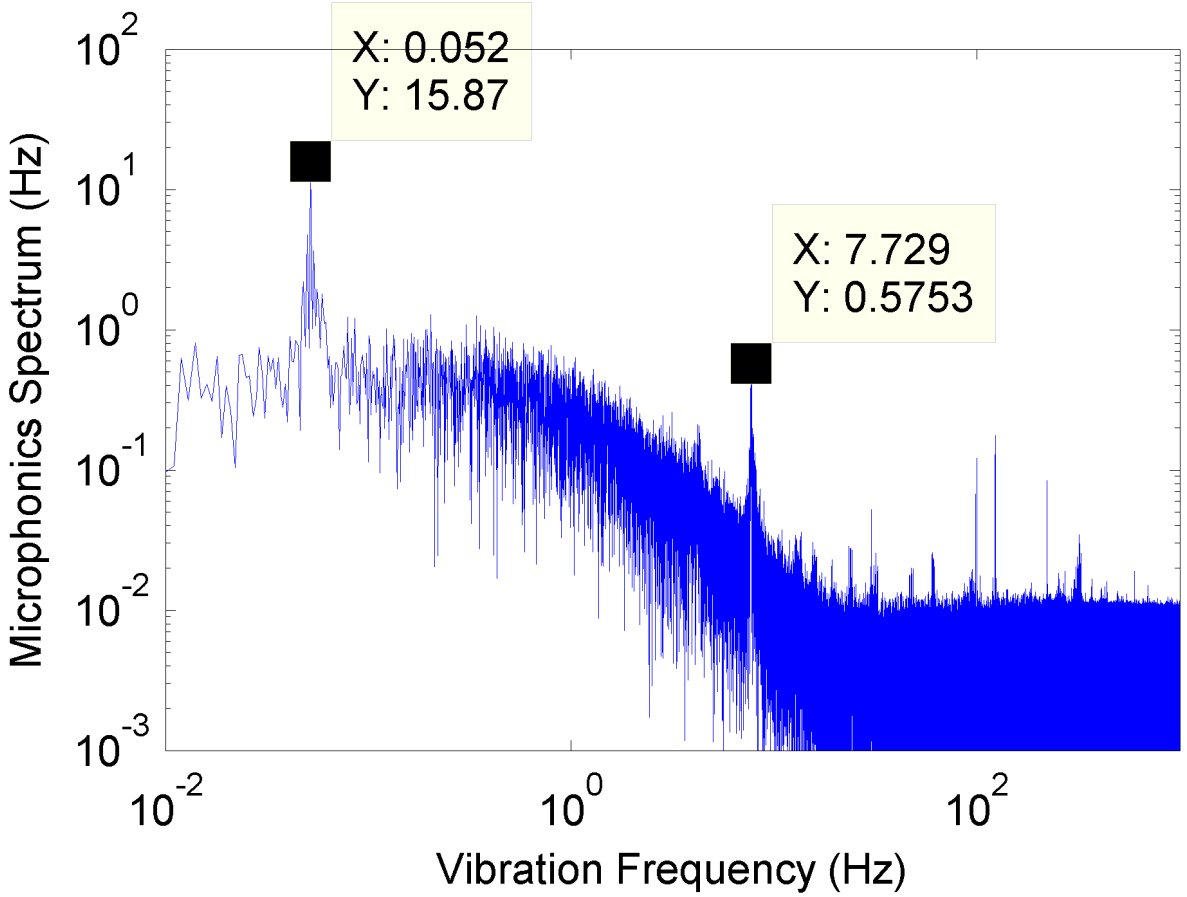

Figure 19 FFT of instant resonant frequency of double spoke cavity (Germaine).The loop amplitude is modulated with a 20-sec period.

8.2 Dynamic Lorentz detuning

One should distinguish between the static and dynamic Lorentz detuning observed during CW and pulsed tests. Contrary to the static one, the dynamic Lorentz force detuning is not restrained effectively by boundary stiffness. In addition, only the dynamic Lorentz force detuning is important for a pulsed system, not the static Lorentz force detuning [16].

A convenient method to determine the coefficients of the dynamic Lorentz force detuning is to modulate the radiation pressure at angular frequency in order to excite one resonant mode only. To this end, one can drive the cavity in CW mode at some relatively high gradient V_0, introduce a small periodic modulation of the cavity voltage and sweep the modulation frequency. This will allow one to measure the amplitude and phase of the cavity frequency modulation as a function of sweep frequency ω, known as the Lorentz transfer function [17].

Several tests were performed at 2 K to find out the optimal parameters of loop, for example, a driven CW mode with a gradient of 5 MV/m, a sweep the modulation frequency with a resolution down to 1Hz. A voltage modulation depth of 25% is set to the start modulation frequency, which will become lower while increasing the modulation frequency. Figure 20 presents the cavity voltage modulation and resonant frequency response in time domain, while Figure 21 gives an example of the modulation frequency and corresponding cavity frequency spectrum at 318 Hz.

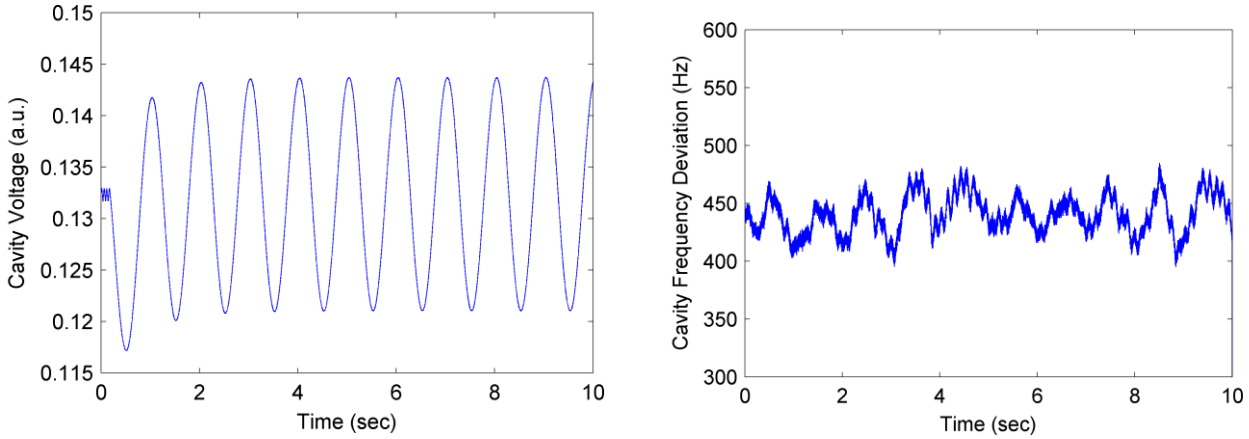

Figure 20 The cavity voltage modulation (left) and resonant frequency responded in time domain (right)

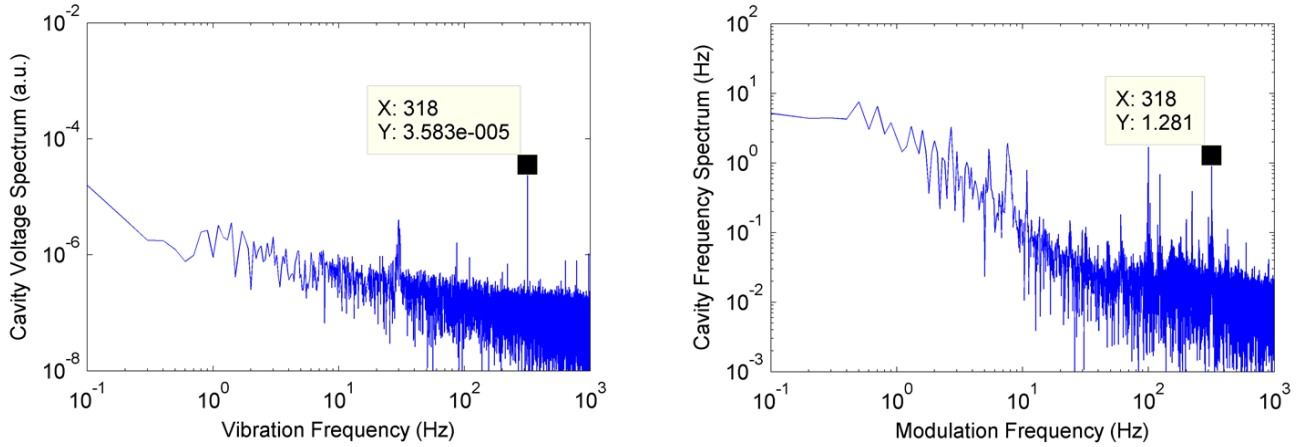

Figure 21 Modulation frequency (left) and corresponding cavity frequency spectrum (right) at 318 Hz

By sweeping the modulation frequency up to 800 Hz, the fit of a multi-peak dynamic Lorentzian curve is shown in Figure 22. Compared to the simulation result from IPNO shown in Table 5, most of the simulation shows a good agreement to the test data. Note that an unexpected harmful frequency of roughly 100 Hz was found in the test. This frequency can be easily excited by the alternative electric frequency of 50Hz, which should be paid a higher attention.

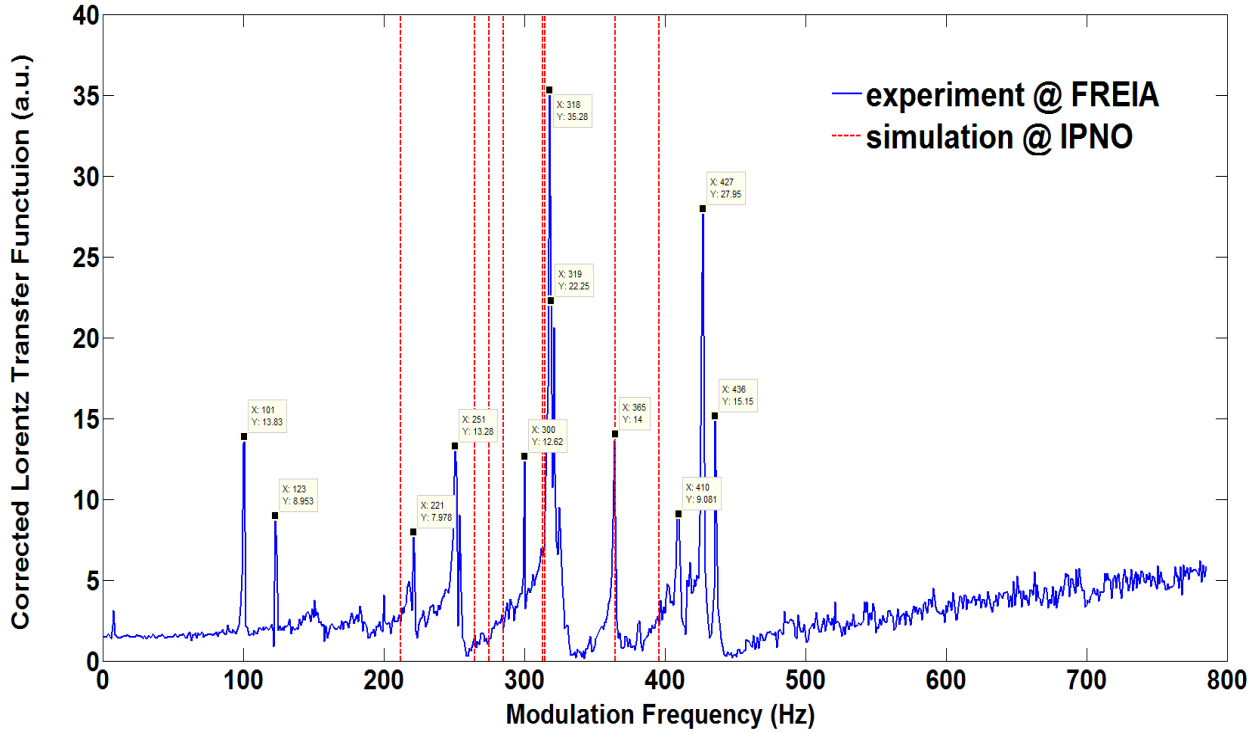

Figure 22 multi-peak dynamic Lorentz force detuning curve of Germaine.

Table 5 The simulation result of dangerous mechanical modes of IPNO

N°	Frequency	Mode
1 & 2	212 Hz	Beam tube on CTS side
3 & 4	265 Hz & 275 Hz	Spoke bar/Helium vessel
5 & 6	285 Hz	Coupled mode Cavity/Helium vessel
7	313 Hz	Helium vessel
8 to 11	315 Hz to 365 Hz	Coupled mode Cavity/Helium vessel
12	396 Hz	beam tubes

9. Microphonics

We studied microphonics both at 2 K and 4 K by operating the cavities in the self-excited loop and monitoring the signal with a Rohde & Schwarz (RTO 1024) oscilloscope with a built-in I/Q demodulation option. Subsequent off-line analysis of the demodulated signal reveals the frequency as a function of time, as shown in Figure 23 and 24. By taking the Fourier transform we finally get the microphonics spectrum from the measurement. A vibration mode of 8 Hz was found in both cases. Next step is to continue investigating where the undesired noise source comes from.

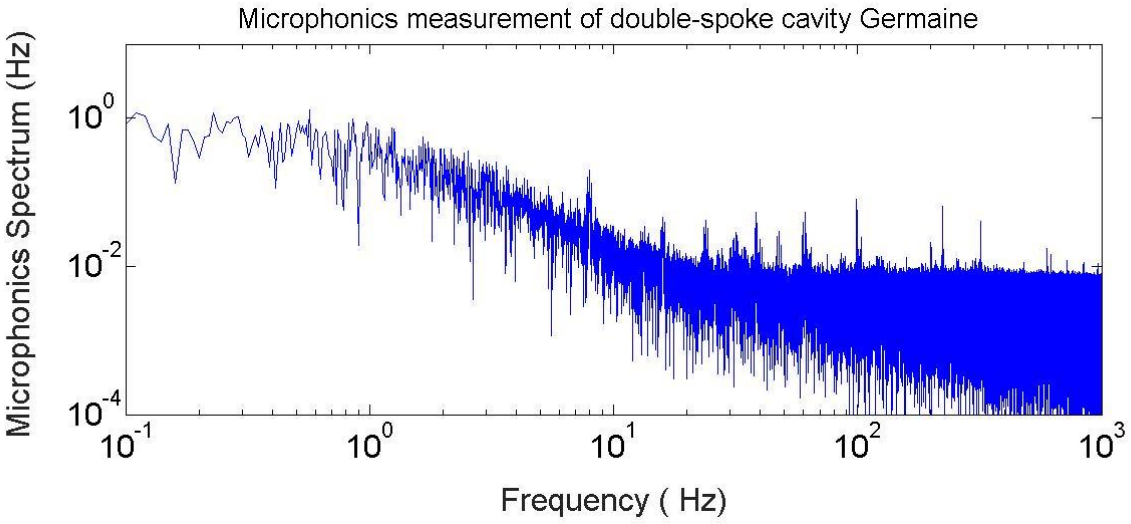

Figure 23 microphonics measurement at 4K_1019_mbar_heat_load_01W

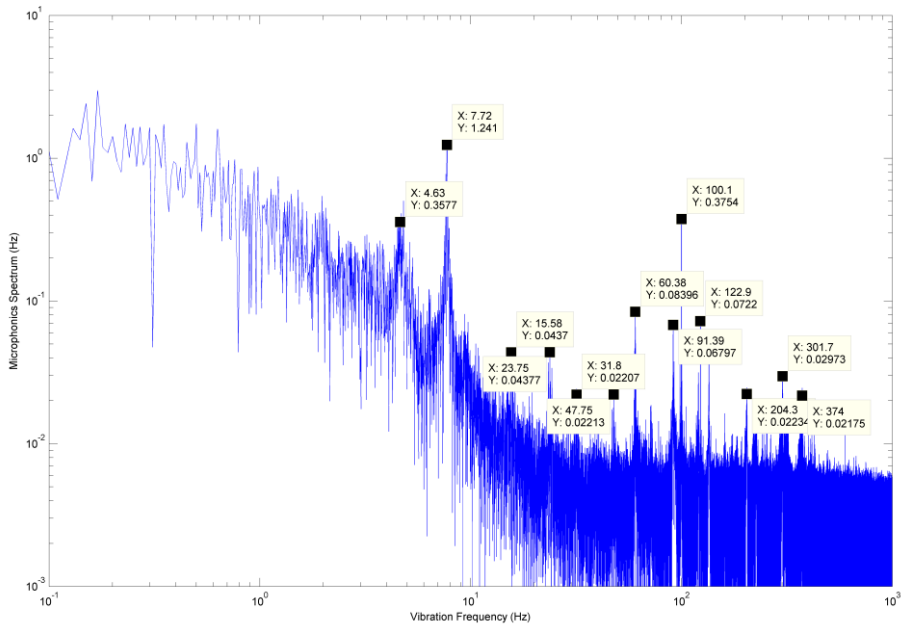

Figure 24 Microphonics measurement at 2K @31mbar. There are 3 main resonances: 4.6; 7.7 and 100 Hz.

10. Tuner sensitivity

The cold tuning system (CTS) is attached to the spoke cavities to adjust the resonant frequency of the cavities in order to counteract the frequency detuning. The spoke CTS integrates two different functions: a slow tuning capability over a wide frequency range by using a step motor; and a fast tuning system by means of piezoelectric actuators inserted in the mechanical system of CTS[18].

The tuning sensitivity could be obtained by formula [19]

$$tuning\quad sensitivity\quad (Hz/mm) = \quad cavity\quad sensitivity \times \left(1 - \frac{1}{1 + K_{CTS}/K_{cavity}}\right) \quad (10.1)$$

Here, K_{CTS} is the required CTS stiffness, while the cavity stiffness would be 20 kN/mm. Given the cavity sensitivity of 110 kHz/mm, the calculated tuning sensitivity will be 135 kHz/mm [18].

Here the behavior of the slow tuning system was studied both at 2 K and 4 K at FREIA, as shown in Figure 25 and 26. A tuning sensitivity of 66 KHz/mm @ 2 K as well as 75.8 KHz/mm @ 4.2 K is learned from the test. With the maximum cavity deformation of 1 mm, the corresponding tuning range by motor is 116.2 kHz @ 4.2 K.

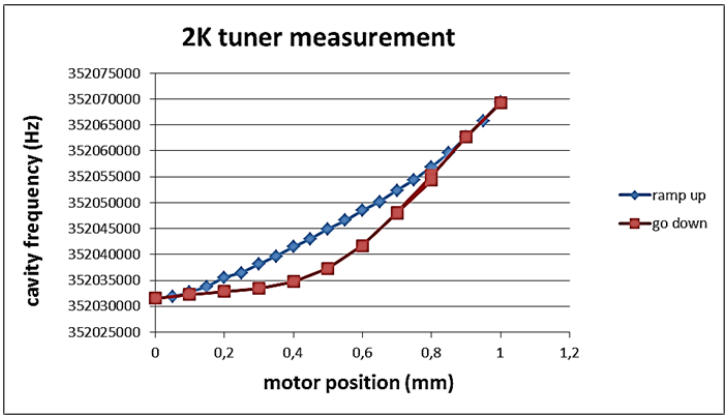

Figure 25 Cavity frequency vs. motor position at 2 K

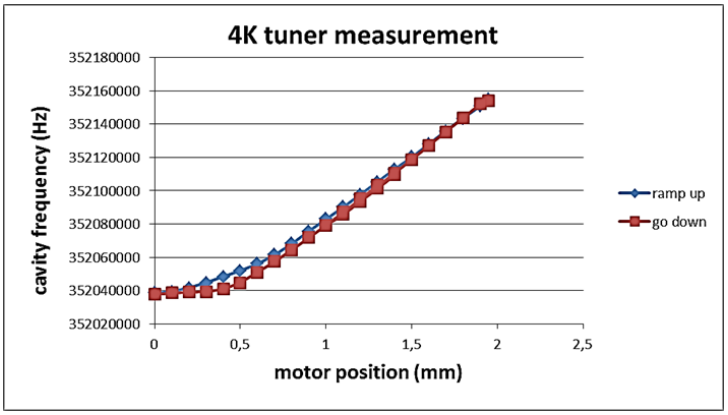

Figure 26 Cavity frequency vs. motor position at 4 K

A comparison with the test curve of IPNO is shown in Figure 27. Though the CTS is installed in a vertical position in IPNO while it is horizontal in HOSS at FREIA, both two results agree with each other quit well.

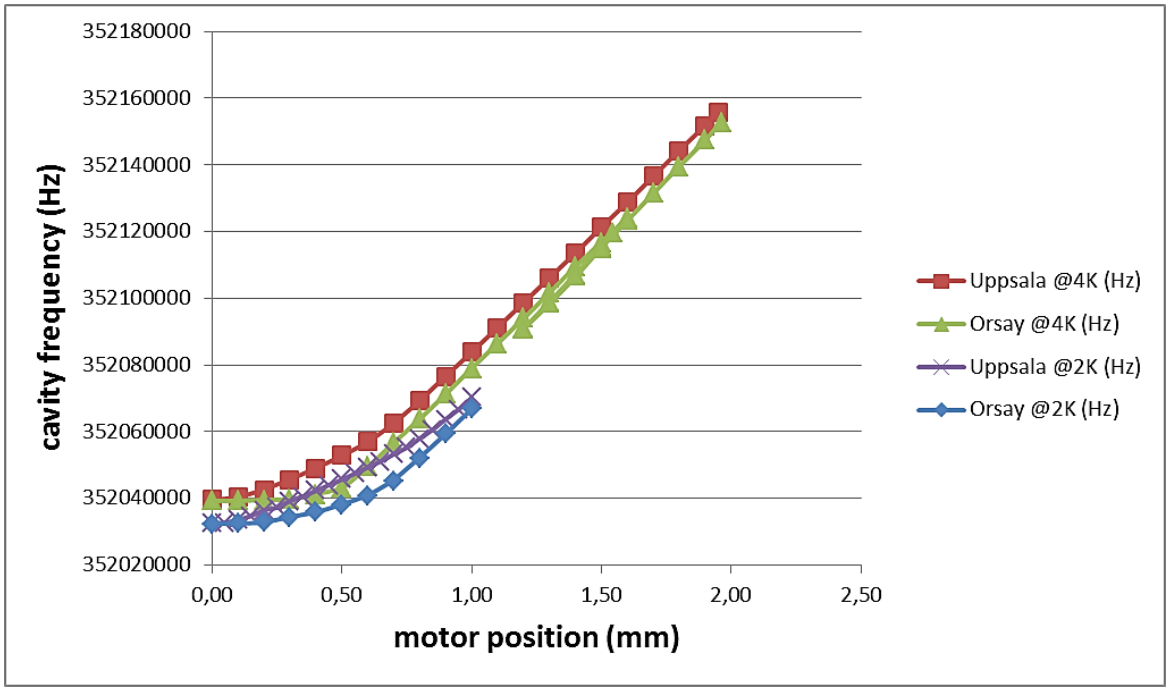

Figure 27 Tuning performance of double spoke cavity's CTS

Also the piezoelectric actuators were measured after charge cycle exercise. All the test data related to the tuning system measurement is listed in Table 6. Similar test results as IPNO's previous test were obtained with FREIA system.

Table 6 CTS summary data table

Cavity ref		SD01	SD01
Name		Germaine	Germaine
cold test date		apr-15	nov-15
Cavity baked ?		No	No
Piezo 1		PI 36 mm	PI 36 mm
Piezo 2		Noliac 50 mm	Noliac 50 mm
Tuner sensitivity @2K	kHz/mm	68,2	66,0
Cavity sensitivity @4K	kHz/mm	72,6	75,8
Tuner sensitivity @300K	kHz/mm	67	-
Cavity sensitivity @300K	kHz/mm	144	-
Fast detuning range P1 @2K	Hz	542	443,0
Fast detuning range P2 @2K	Hz	791	544,0
Frequency @4K (w/o tuner)	MHz	352,038	352,038
Frequency @2K (w/ tuner)	MHz	352,032	352,032
Pressure sensitivity w/o tuner	Hz/mbar	5,5	5,0
Pressure sensitivity w tuner	Hz/mbar	14,5	--
Lorentz sensitivity w/o tuner	Hz/(MV/m²)	-8,1	-6,8

11. Summary

The first step of a test stand based on a self-exited loop was developed at FREIA. The first cavity for the ESS project we tested was a bare double spoke cavity Germaine, which was designed and built by IPN Orsay. The RF performance and mechanical behavior of the cavity at low power level was studied extensively at FREIA. Similar test results as IPNO's previous tests were obtained with the FREIA system. In the next step, the spoke cavity with a RF power coupler will be tested at high power in the horizontal cryostat with the tetrode based RF system.

References

[1] Steve Peggs, Conceptual design report, 2012.

[2]] P. Duchesne et al., "Design of the 352 MHz, Beta 0.50, double-spoke cavity for ESS", SRF 2013, FRIOC01.

[3] R. Ruber et al., "The New FREIA Laboratory for Accelerator Development", Proceedings

IPAC'14, Dresden, Germany (2014) THPRO077.

[4] Roger Ruber et al., "Uppsala test facility project plan. Uppsala University", FREIA report 062013/3.

[5] "CNRS and ESS Advance a New Standard for Linac Design", Last modified September 30, 2015.

https://europeanspallationsource.se/sites/default/files/spoke_cavities_wp4_pdf_0.pdf.

[6] "Spoke RF", Accessed January 20,2016. https://europeanspallationsource.se/spoke-srf.

[7] P. Duchesne et al., "Design of the 352 MHz, Beta 0.50, double-spoke cavity for ESS", SRF 2013, FRIOC01.

[8] Guillaume OLRY, "Spoke Cryomodules (WP4)", Last modified April 21, 2015.

https://indico.esss.lu.se/event/316/contribution/17/material/1/1.pdf.

[9] Jean Delayen. "Self-exited loop", Jefferson lab LLRF workshop, 2001.

[10]Han Li, et,al. "Test Characterization of Superconducting Spoke Cavities at Uppsala university", SRF2015,TUP083.

[11] R. Santiago Kern et al., "The HNOSS horizontal cryostat and helium liquefaction plant at FREIA", IPAC 2014, WEPRI110.

[12]Han Li, et,al. " RF Test of the Hélène Single Spoke Cavity", FREIA report, 112015/10.

[13]V.A. Goryashko et al., "method for high-precision characterization of the Q-slope of superconducting RF cavities", submitted to Transactions on Microwave Theory and Techniques.

[14]J. Bardeen et al., "Theory of superconductivity", Phys.Rev. 108 (5) (1957) 1175.

[15]Hasan Padamsee et al., RF superconductivity for accelerators, 88-89.

[16] R. Mitchell K. Matsumoto et al., "Lorentz force detuning analysis of the spallation neutron source (sns) accelerating cavities", Proc. of the10th Workshop on RF Superconductivity(2001) ,236.

[17] V.A. Goryashko, "An approach to characterization of the Lorentz transfer function of ESS spoke cavities at FREIA", FREIA report, 052014/5.

[18]N. Gandolfo et al., "Reynet Deformation tuner design for a double Spoke cavity", SRF 2013, THP078.

[19]Steve Peggs, ESS technical design report,2013, 321.